Ultrabroadband spectral amplitude modulation using a liquid crystal spatial light modulator with ultraviolet-to-near-infrared bandwidth

Jiangfeng Zhu,* Takashi Tanigawa, Tao Chen, Shaobo Fang, Keisaku Yamane, Taro Sekikawa, and Mikio Yamashita

Department of Applied Physics, Hokkaido University, and Core Research Evolutional Science and Technology, Japan Science and Technology Agency, Kita-13, Nishi-8, Kita-ku, Sapporo, 060-8628, Japan

*Corresponding author: jfzhu@eng.hokudai.ac.jp

Received 11 November 2009; accepted 2 December 2009;
posted 4 December 2009 (Doc. ID 119866); published 12 January 2010

The first demonstration to our knowledge in the spectral range from 300 to 1100 nm is presented for the amplitude modulation characteristics of a two-channel 648-pixel liquid crystal spatial light modulator. The broadest spectral amplitude modulation for UV (380–420 nm) and visible-to-near-IR (500–900 nm) pulses to generate a spectral-shifted pulse pair is experimentally realized. The results show that the liquid crystal spatial light modulator has a potential application for attosecond extreme-UV pulse characterization with the conventional SPIDER algorithm and the capability to shape monocycle optical pulses.

OCIS codes: 230.6120, 320.5540, 320.7100, 320.7160.

1. Introduction

Liquid crystal spatial light modulators (LC-SLMs) have been extensively used for femtosecond pulse shaping and nonlinear chirp compensation for the past ten years because of their flexibility for adaptive computer programming control [1–3]. Although acousto-optic modulators [4,5] can also realize adaptive programming control as narrowband tunable filters and narrowband phase modulators, bulk TeO_2 crystal is prevented from handling ultrashort pulses that approach few cycle to monocycle and contain an ultrabroadband spectrum because of the large incompletely compensated higher-order dispersion. Moreover, the throughput efficiency of the acousto-optic modulator decreases rapidly with the increase of the spectral bandwidth, typically less than 10% over a 450 nm spectral width. In addition, the several-centimeter-long acousto-optic crystal [6] cannot bear the high peak power because of self-phase modulation (SPM), and the small aperture limits the achievable pulse energy, so it can not be applied to high-energy few-cycle-to-monocycle optical pulses. On the other hand, the LC-SLM has the advantage of a much larger bandwidth (typically spanning more than one octave), much lower dispersion, and higher efficiency compared with the programmable acousto-optic modulator. Therefore it is extraordinarily suitable for pulse shaping and nonlinear chirp compensation of an ultrabroadband spectrum generated directly from a Ti:sapphire oscillator emitting octave-spanning spectra [7,8], by SPM and/or induced phase modulation in a gaseous media [9–11], or multiple Raman processes [12,13], which typically cover more than a one- or two-octave spectrum from UV to near-IR (NIR). The LC-SLM paves the way for coherent synthesis of single-cycle optical pulses and coherent control of atoms and molecules. Recently, 2.6 fs single isolated optical pulses, which contain only 1.3 optical cycle, were generated by nonlinear chirp compensation of the spectrum broadened by SPM as well as induced phase modulation in an argon-gas-filled hollow fiber by using an

0003-6935/10/030350-08$15.00/0

LC-SLM [14]. These are till now the shortest isolated optical pulses generated in the visible range, which shows the powerful capability of phase modulation of the LC-SLM. More recently we fabricated a UV-transparent LC-SLM [15], and the UV pulses generated by frequency doubling of the laser pulses from a Ti:sapphire amplifier were shortened to their near-Fourier-transform-limited pulse duration through feedback chirp compensation [16], which means that the applicable spectral range of the LC-SLM has been extended to the UV region.

Besides phase modulation, the LC-SLM has an application for arbitrary amplitude modulation in the frequency domain to generate an arbitrary spectral shape. It can be used as a flexible bandpass filter to optimize the ultrabroadband spectrum generated by SPM by removing the fine structure. Amplitude modulation using the LC-SLM is also very important in various fields such as pump–probe experiments to study selective absorption of organic or biological molecules. The ultrabroadband characteristics of the LC-SLM allow it to be applied for shaping few-cycle-to-monocycle intense pulses for driving single attosecond pulse generation [17–20]. In particular, when preparing a spectral-shifted and time-delayed driving pulse pair by amplitude modulation, we believe it is promising to realize attosecond pulse characterization in the extreme-UV (XUV) wavelength region by using the conventional SPIDER algorithm with the great ability of the single-shot measurement [21–23], avoiding the challenge to directly generate two frequency-shifted and time-delayed harmonic pulses. The first experimental complete temporal characterization of high-harmonic XUV pulses by this technique was carried out by use of a programmable acousto-optic filter to tailor the IR pulses to deliver two replicas delayed by τ and with a spectral shift $\delta\omega$ [24]. However, because of the narrow bandwidth and large dispersion of the acousto-optic device and the gain narrowing effect in the amplification stage, the driving pulse replica has a duration as long as 50 fs, which can generate only discrete odd-order XUV spectra and, therefore, a discrete XUV pulse train. In order to characterize isolated single attosecond XUV pulses by the SPIDER method, one must employ a few-cycle-to-monocycle pumping pulse pair to generate continuous XUV spectra with a proper spectral shift. The LC-SLM is a superior candidate to accomplish this task, benefiting from its ultrabroadband characteristics and active phase and amplitude modulation [25,26].

In this paper, we report for what we believe to be the first time the amplitude modulation characterization of a two-channel 648-pixel UV–NIR LC-SLM. The relationship between the transmittance and the phase modulation was studied and used in the computer program. Next we experimentally realized ultrabroadband amplitude modulation to generate spectral-shifted UV and visible-to-NIR pulse pairs, indicating that the UV-NIR LC-SLM is a promising tool for generating a few-cycle-to-monocycle spectral-shifted pulse pair for the attosecond SPIDER measurement.

2. Characterization of Amplitude Modulation

The structure of the 648-pixel LC-SLM with two channels is the same with that described in [16]. The effective surface of the LC-SLM was 20 mm× 65 mm, and the pixel width was 98 μm with a pixel gap of 5 μm. The LC was sandwiched between two 0.7 mm thickness fused-silica substrates, which were antireflection coated for high transmission from UV to NIR. The thickness of the LC layer was designed to be 20.0 μm. The orientations of the LC molecules of both surfaces were made parallel to each other by the use of the oriented organic films. In order to achieve the effective transmission in the UV region, a new kind of LC molecule with a mixture of cyclohexane derivatives with fluorine substituents was employed [27]. Moreover, the thickness of the transparent conductive indium tin oxide was as thin as 100 nm to minimize the transmission loss in the UV wavelengths. The LC-SLM's transmission edge in the UV region is below 300 nm and is over 50% transmittance at above 315 nm, while in most of the wavelength range from 400 to 1600 nm the transmittance is around 80%–90%. The optical and dielectric anisotropies are 0.08 (the extraordinary refractive index $n_e = 1.564$) at 589 nm and 4.7 (the dielectric constant of the minor axis direction $\varepsilon_\perp = 3.7$) at 1 kHz, respectively.

In order to investigate the performance of amplitude modulation of the LC-SLM, it was located between two parallel-placed broadband polarizers while keeping the orientation of the LC molecule at 45° with respect to the direction of the polarizers. In the visible-to-NIR region, a halogen lamp was used as the light source, and below 400 nm it was replaced by a xenon lamp. A monochromator with an intensified CCD (ICCD) was employed to record the transmitted spectral intensity. We applied the AC-like electric waveform with an amplitude of 5 V and a pulse duration of 2.73 ms on the two sides of the LC-SLM. The applied pulse width was changed with the 8 bit resolution [256 gray-scale levels (X)]. Under the applied electric pulses, the extraordinary refractive index ($n_e(\lambda, X)$) of the LC changes correspondingly while the ordinary refractive index ($n_o^c(\lambda)$) remains constant [16], so that the polarization state of the input light changes after passing through the LC-SLM. According to the Jones matrix calculation, the output transmittance of such an optical system can be described as

$$T(\lambda, X) = \frac{1}{2}\{1 + \cos[\varphi_{\text{offset}}(\lambda) - \varphi(\lambda, X)]\}. \quad (1)$$

We define $\varphi_{\text{offset}}(\lambda) = 2\pi d[n_e^c(\lambda) - n_o^c(\lambda)]/\lambda$ as the offset phase, where $n_e^c(\lambda) = 1.5438 + 7093/\lambda^2$ and $n_o^c(\lambda) = 1.4676 + 6132/\lambda^2$ are the Sellmeier equations of the LC material and $d = 20.0\,\mu$m is the thickness of the LC. The second term

$\varphi(\lambda, X) = 2\pi d[n_e(\lambda, X) - n_e(\lambda, X = 0)]/\lambda$ stands for the phase modulation as a function of the gray scale X and the wavelength λ. Our previous study [15,16] has shown that the phase modulation is expressed as a product of the normalized phase modulation $g_N(X)$ (wavelength-independent) and the gray-scale-independent dispersion function $f(\lambda)$; that is, $\varphi(\lambda, X) = g_N(X)f(\lambda)$, which makes computer control easier.

We measured experimentally the amplitude modulation with the gray scale from 0 to 255 in the wavelength range from 300 to 1100 nm, which spans nearly two octaves. The result is shown in Fig. 1. In addition, the phase modulation characteristics of this LC-SLM were also measured based on the technique of the channeled spectrum [28]. Figure 2(a) shows the gray-scale-independent dispersion function $f(\lambda)$. We can see that the phase modulation increases with the decrease of the wavelength because of the normal dispersion characteristics of the LC material. Even in the longest wavelength at 1100 nm, the maximum phase change is over 2π, which means that arbitrary amplitude modulation can be realized, as shown in Eq. (1). Figure 2(b) is the wavelength-independent, normalized phase modulation $g_N(X)$, which is valid in the wavelength range from UV to NIR. Substituting these data into Eq. (1), we can calculate the transmittance with the wavelength and the gray scale. Finally we found that there is excellent coincidence between the measured transmittance and the calculated one. Figure 3 shows the comparison of the transmittance between the measurement and the calculation at four different wavelengths from 350 to 1000 nm. The deviation at most gray-scale levels is less than 5% except for the fast oscillating area. At the small gray-scale region (0–25) at 350 and 400 nm, the deviation is much larger, which may result from the fact that the imperfect response of the orientation of the LC molecule is sensitive to the applied electric waveform in the UV wavelength region in this gray-scale region. However, we can ignore these deviations because we never use these gray scale levels. The maximum transmittance of slightly less than 80% at 1000 nm may be due to the quality of the antireflection coating

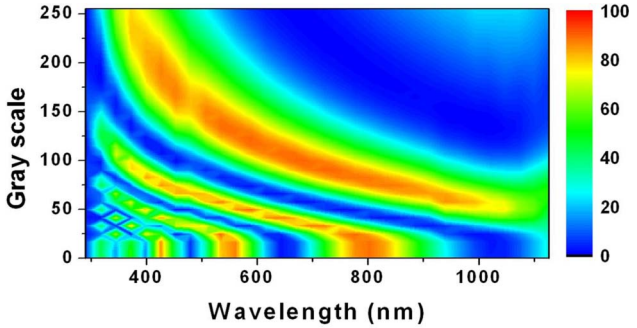

Fig. 1. (Color online) Contour map of the measured transmittance with wavelength from 300 to 1100 nm and gray-scale levels from 0 to 255.

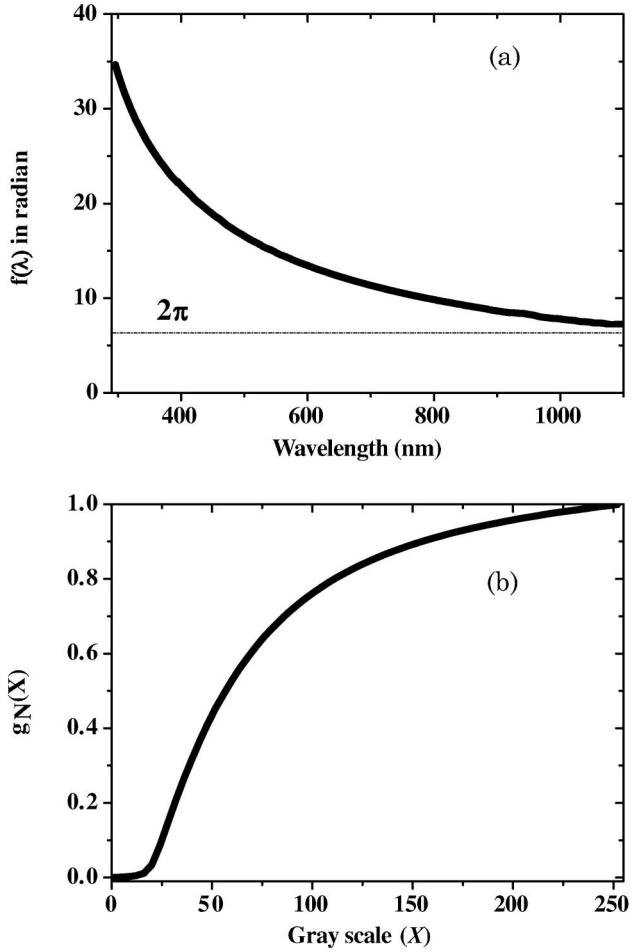

Fig. 2. Phase modulation characteristics of the LC-SLM. (a) Gray-scale-independent dispersion function with the wavelength from 300 to 1100 nm. (b) Normalized wavelength-independent phase modulation with gray scale from 0 to 255.

in the NIR region. The good consistence between the measurement and the calculation confirmed that we can use the transmittance formula to make the computer program, which is simple, rapid, and precise.

Let us look at Figs. 1 and 3 again. There are more and more transmittance oscillation numbers with decreasing wavelength. There are almost six periods at 300 nm. Each transmittance oscillation means that the phase modulation varies with a period of 2π. This property tells us that the resolution of the transmittance is wavelength dependent. At longer wavelengths, there are more modulation steps, which means that a higher modulation resolution can be achieved. While at shorter wavelengths there are more transmittance oscillations, we had better choose the higher gray-scale region to obtain as high a resolution as possible.

Note that in Fig. 2(b) there is a threshold gray scale for initiating the phase modulation, and from it we can derive the elastic constants of the new LC based on the Freedericksz transition method [29], where $k_{11} = (V_c/\pi)^2 \cdot \Delta\varepsilon \cdot \varepsilon_0$ and $k_{33} = k_{11}(\kappa + 1)$. Here V_c is the threshold electric voltage,

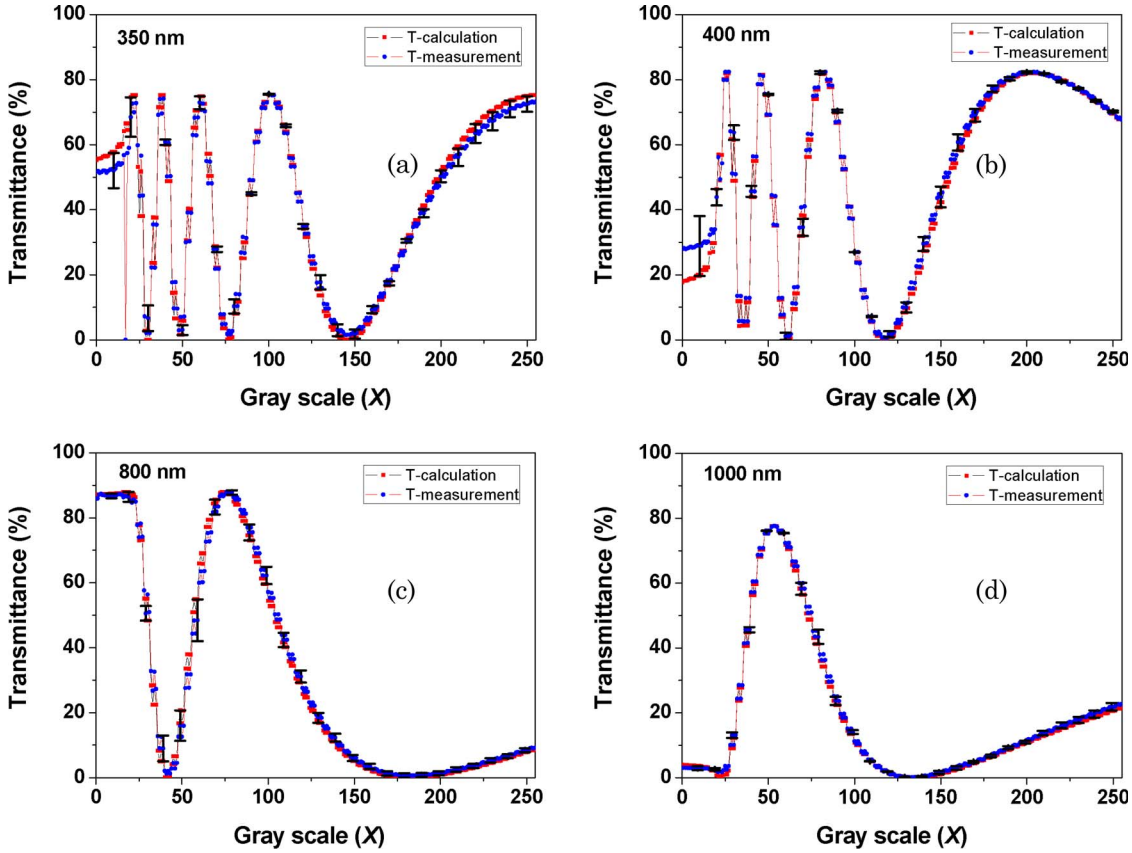

Fig. 3. (Color online) Measured and calculated transmittance at four different wavelengths from UV to NIR. The error bar depicts the difference between the measurement and the calculation.

$\Delta\varepsilon$ is the dielectric anisotropy, ε_0 is the dielectric constant, and κ is the fitted slope of the normalized phase modulation. The splay elastic constant k_{11} is calculated to be 10.8×10^{-12} N, and the bend/splay elastic constant ratio k_{33}/k_{11} is 2.74. These elastic constants measured by this optical method agree well with those measured by the conventional voltage–capacitance method, where $k_{11} = 10.1 \times 10^{-12}$ N and $k_{33}/k_{11} = 2.79$ [30]. The precision of this measurement method was confirmed to be about $\pm 5\%$. The elastic constants are very important for us to learn more about the physical properties of the LC molecule; especially the elastic constant ratio k_{33}/k_{11} strongly affects the static and dynamic performance of the LC [29].

3. Experiments for Spectral Pair Generation and Discussion

To study the feasibility of amplitude modulation in the UV–NIR spectral range by the LC-SLM, we performed two experiments: one was for the UV spectrum in the 400 nm range, and the other was for the supercontinuum spectrum by SPM in the visible-NIR range. The experimental setup is depicted in Fig. 4. A femtosecond Ti:sapphire amplifier (Femtopower 1000, Femtolasers GmbH) was utilized as the laser source, which can output 350 μJ, 30 fs laser pulses at a 1 kHz repetition rate. For the second-harmonic generation, a 10 μm thickness type I BBO crystal was employed, and the average output power at 400 nm is 20 mW with a spectral bandwidth of about 10 nm (FWHM). For the supercontinuum generation, the 350 μJ laser pulses from the Ti:sapphire amplifier were loosely focused into a hollow fiber (core diameter 300 μm, length 0.5 m), and the broadband spectrum covered from 500 to 900 nm with a throughput efficiency of about 40% when filled with 1.5 atm Ar gas. A half-wave plate was placed before the $4f$ system to rotate the input polarization of the laser pulses by 45° with respect to the orientation of the LC molecule for amplitude modulation. The LC-SLM was located on the Fourier plane of the $4f$ system and was controlled by a personal computer. The $4f$ system was precisely aligned to minimize the temporal and spatial chirp. Because of the somewhat narrow bandwidth of the UV pulses, we selected high-groove-density Al-coated gratings (a groove density of 1200 lines/mm) and Al-coated concave mirrors with a large radius of curvature (ROC = 700 mm) to fully disperse the spectrum. For the supercontinuum spectrum, the gratings were replaced with Au-coated 300 lines/mm ones and the concave mirrors with Ag-coating and ROC of 500 mm. After the $4f$ system a broadband polarizer was used to filter out the useful spectrum and was recorded by a monochromator with an ICCD. The spectral resolution of the monochromator is 0.04 nm for the UV spectrum and 0.45 nm for the

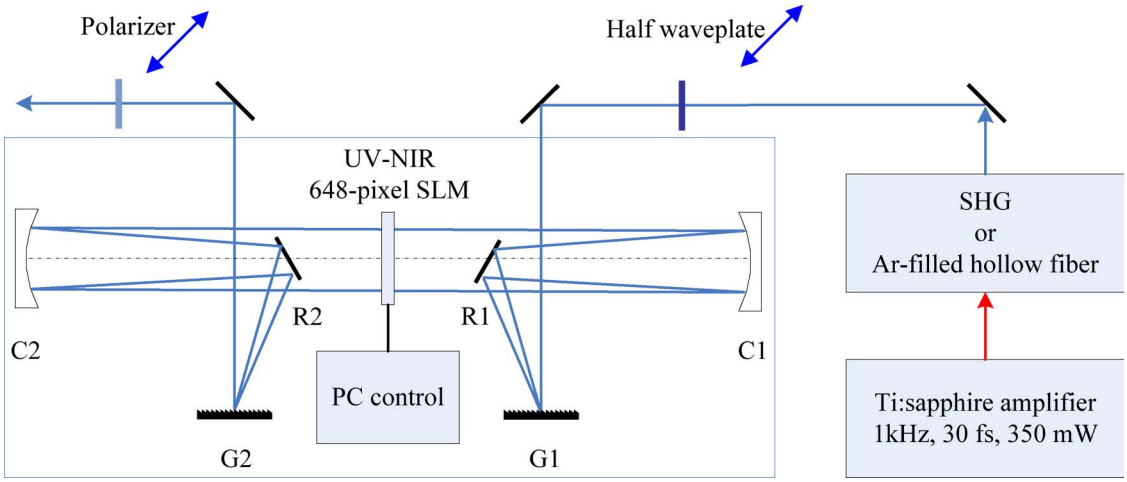

Fig. 4. (Color online) Schematic of the experimental setup. SHG, second-harmonic generation; G1, G2, grating; R1, R2, Al-coated reflective mirror; C1, C2, concave mirror.

broadband supercontinuum spectrum achieved by automatically changing the gratings with different groove densities.

As described above, the LC-SLM has the capability of arbitrary amplitude modulation from 300 to 1100 nm; thus we can modulate the spectrum to any shape, for example, a rectangular shape or a Gaussian shape, and any intensity, regardless of the available pulse energy. We are especially interested in generating a few-cycle-to-monocycle pulse pair with a proper spectral shift for the application of attosecond SPIDER. As a result, as the first step toward this purpose we would like to generate arbitrary frequency-shifted spectra in the UV–NIR range. Straightforwardly one can modulate the original spectrum to a rectangular or a Gaussian shape spectral pair with slightly different central wavelengths, which was accomplished in [24] by use of an acousto-optic modulator. However, considering the complex structure of the ultrabroadband spectrum produced by SPM, it is very difficult to get a smooth rectangular or Gaussian shape spectral pair, or at least lose most of the pulse energy by filtering the useless spectral component. We find that by introducing a small spectral shift while preserving the original spectral profile through amplitude modulation using the LC-SLM, the highest throughput can be fulfilled. We have to stress that there is no real spectral shift by means of nonlinear frequency mixing, but the apparent spectral shift is obtained by amplitude modulation of the original spectrum to the short and long central wavelengths. This is equivalent to an actual spectral shift and is essential for the spectral-shifted XUV pulse pair generation that was done in [24].

Figure 5 shows the experimental results of amplitude modulation for the generation of an arbitrary spectral-shifted pulse pair in the UV and visible-NIR region. For the second-harmonic pulses, the frequency shift $\Omega/2\pi$ is set as 1.59 THz, and for the SPM pulses it is 3.18 THz. Figures 5(a) and 5(c) are the modulated spectra of the UV pulses from 380 to 420 nm and the SPM pulses from 500 to 900 nm, respectively. Insets are the calculated Fourier-transform-limited pulse durations, which are 20.0 fs for the UV spectrum and 4.8 fs for the SPM spectrum, respectively. It is clear that by amplitude modulation, a spectral-shifted pulse pair with the central wavelengths shifted toward short and long wavelengths was produced while keeping the envelope the same structure as its original spectrum. To the best of our knowledge, the latter result shows that the broadest spectral amplitude modulation has been achieved by using one LC-SLM. The weighted central wavelength of the UV spectral pair is 401.7 and 402.5 nm, while it is 704.0 and 710.2 nm for the supercontinuum spectral pair. These results agree well with the values preset through the computer program in the experiments. Note that in Fig. 5(c), it seems that the spectral shift is not so obvious in the short wavelength region from 550 to 650 nm than that in the longer-wavelength region. One reason is that the spectral intensity is relatively low and the spectrum is smooth enough. The other reason is that the spectral shift is inversely proportional to the wavelength, so that it seems more notable in the long wavelength range than that in the short wavelength range. The precision of amplitude modulation is limited by the finite resolution of the 8 bit gray-scale levels with an ambiguity of less than 5%. If we further increase the resolution of the gray scale to 10 bits or even higher, which is in progress, better precision of amplitude modulation may be achieved with an uncertainty less than 1%. Figures 5(b) and 5(d) are the corresponding gray scales on the pixels of the LC-SLM to achieve the desired transmittance. For the UV spectrum, 185 pixels were used, and the wavelength resolution was 0.2 nm/pixel. For the SPM spectrum the effectively used pixel number was 260, and the wavelength resolution was 1.3 nm/pixel. By properly choosing the groove density of the gratings and the ROC of the concave mirrors, one can make full use of the 648 pixels of the LC-SLM to achieve the highest wavelength

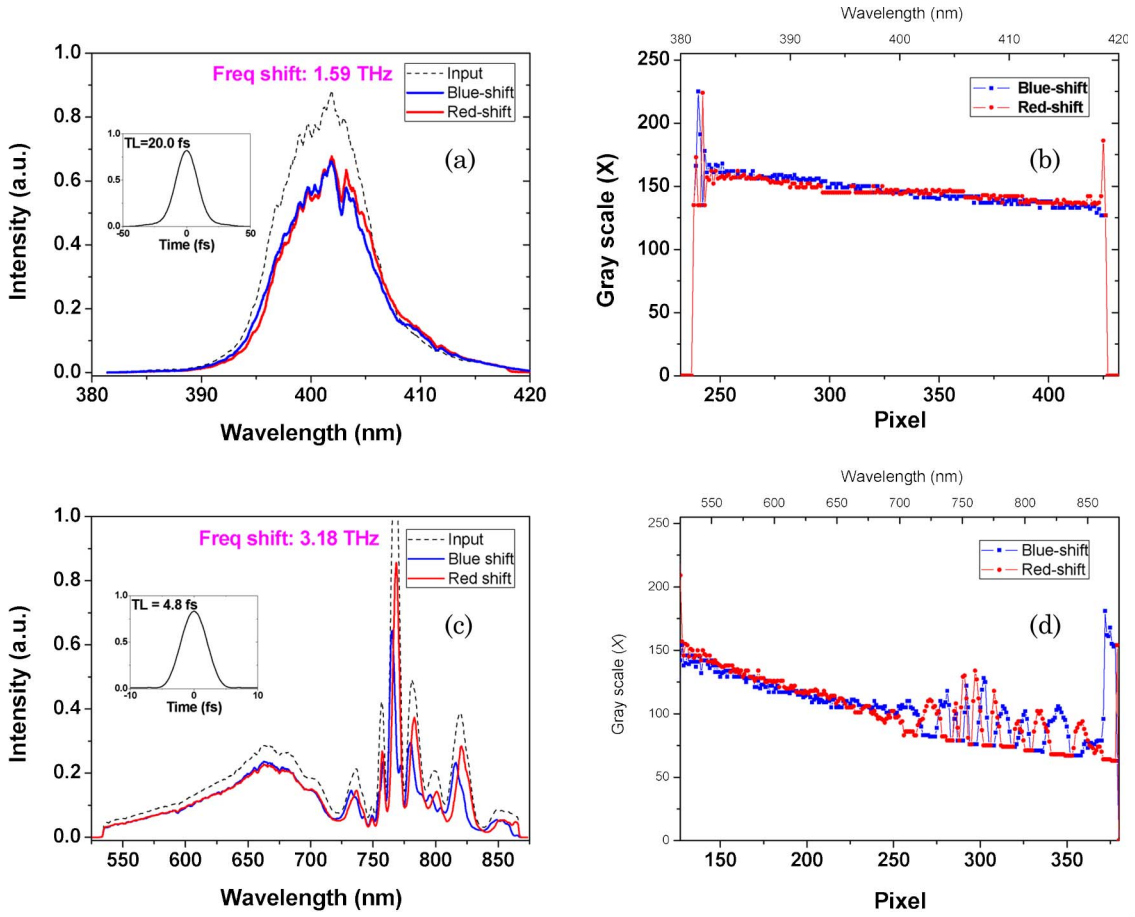

Fig. 5. (Color online) Spectral-shifted pulse pair generation in the UV (a) and visible-to-NIR region (c). Dashed curve, the input spectrum; inset, calculated Fourier-transform-limited (TL) pulse duration. (b), (d), corresponding gray scales on each pixel.

resolution, in other words, the highest amplitude modulation resolution.

The experimental results indicate that the LC-SLM can be used for arbitrary amplitude modulation from UV to NIR, while the spectral bandwidth of the acousto-optic modulator is much narrower not only in the visible-to-NIR region [5] but also in the UV region [6] than that of the LC-SLM. Even a specially designed acousto-optic programmable dispersive filter (DAZZLER, Fastlite) can only cover a wavelength range as broad as 350 nm [31]. It is impossible to achieve greater than a one-octave-spanning spectral bandwidth. With the decrease of the wavelength to the UV range, the bandwidth of the acousto-optic modulator is further decreased, mainly due to the increase of the dispersion, and the diffraction efficiency is reduced accordingly. Owing to the ultrabroadband characteristics of the LC-SLM, it has the remarkable advantage of phase and amplitude modulation of fewcycle-to-monocycle pulses that span approximately one octave for single isolated attosecond pulse generation and characterization. We can prepare the pulse pair with a time delay and a spectral shift by combination of the phase modulation and amplitude modulation LC-SLMs, in which the phase modulation LC-SLM is used for nonlinear chirp compensation and the amplitude modulation LC-SLM for spectral shift generation. The time delay can be realized either by the delay line or by the phase modulation LC-SLM, since it can easily produce an arbitrary group delay. We are now carrying on the fabrication of two-channel dual-LC-SLM, which contains an amplitude modulation LC-SLM and a phase modulation LC-SLM. We plan to realize the arbitrary spectral shift generation and nonlinear chirp compensation simultaneously with an ultrabroadband supercontinuum spectrum generated by SPM and induced phase modulation that covers the 300–1100 nm spectral range. Furthermore, the large effective surface of the LC-SLM with two channels permits high-energy illumination without degradation of the LC material, while for the acousto-optic modulator the achievable pulse energy is limited by the small aperture. One can modify the $4f$ system by replacing the concave mirrors with cylindrical mirrors to enlarge the beam size on the LC-SLM and therefore reduce the peak intensity. By investigating the optical damage threshold of the LC-SLM using 30 fs, 790 nm laser pulses at a repetition rate of 1 kHz with an intensity of 29.6 GW/cm^2 and their second-harmonic pulses with an intensity of 1.3 GW/cm^2 for longer than 1 h, we deduce that the full area of the LC-SLM can bear as high as 3.6 mJ, 2.5 fs, 1 kHz repetition rate laser pulses

[16]. Typically the overall throughput of the $4f$ system based on silver mirrors including the LC-SLM is below 30%. However, it has been reported that by carefully choosing the optics in the $4f$ system, as high as 50% throughput has been obtained and the available pulse energy is 0.5 mJ [32], which is sufficient for driving the attosecond pulse generation. This allows us to carry out the experiment of the attosecond pulse generation and characterization by the proposed method under the present laser conditions.

4. Conclusion

In conclusion, we have studied the amplitude modulation characteristics of a two-channel 648-pixel LC-SLM that is transparent from 300 to 1600 nm. It was found that the calculated transmittance based on phase modulation agrees well with the measured transmittance. As a result, we can control the arbitrary amplitude modulation through the computer program using a simple equation. The broadest amplitude modulation for the spectral-shifted pulse pair generation of the UV pulses (from 380 to 420 nm) and the supercontinuum pulses (from 500 to 900 nm) was realized experimentally by one LC-SLM. This verified the capability of the LC-SLM for arbitrary amplitude modulation in the UV–NIR spectral range, so that it is a superior candidate for arbitrary amplitude modulation of few-cycle-to-monocycle optical pulses for the isolated attosecond pulse characterization using the conventional SPIDER algorithm.

References

1. A. M. Weiner, "Programmable shaping of femtosecond optical pulses by use of 128-element liquid crystal phase modulator," IEEE J. Quantum Electron. **28**, 908–920 (1992).
2. A. Efimov, C. Schaffer, and D. H. Reitze, "Programmable shaping of ultrabroad-bandwidth pulses from a Ti:sapphire laser," J. Opt. Soc. Am. B **12**, 1968–1980 (1995).
3. A. M. Weiner, "Femtosecond pulse shaping using spatial light modulators," Rev. Sci. Instrum. **71**, 1929–1960 (2000).
4. P. Tournois, "Acousto-optic programmable dispersive filter for adaptive compensation of group delay time dispersion in laser systems," Opt. Commun. **140**, 245–249 (1997).
5. F. Verluise, V. Laude, Z. Cheng, Ch. Spielmann, and P. Tournois, "Amplitude and phase control of ultrashort pulses by use of an acousto-optic programmable dispersive filter: pulse compression and shaping," Opt. Lett. **25**, 575–577 (2000).
6. S. Coudreau, D. Kaplan, and P. Tournois, "Ultraviolet acousto-optic programmable dispersive filter laser pulse shaping in KDP," Opt. Lett. **31**, 1899–1901 (2006).
7. R. Ell, U. Morgner, F. X. Kartner, J. G. Fujimoto, E. P. Ippen, V. Scheuer, G. Angelow, T. Tschudi, M. J. Lederer, A. Boiko, and B. Luther-Davies, "Generation of 5 fs pulses and octave-spanning spectra directly from a Ti:sapphire laser," Opt. Lett. **26**, 373–375 (2001).
8. T. R. Schibli, O. Kuzucu, J. Kim, E. P. Ippen, J. G. Fujimoto, F. X. Kaertner, V. Scheuer, and G. Angelow, "Toward single-cycle laser systems," IEEE J. Sel. Top. Quantum Electron. **9**, 990–1001 (2003).
9. S. Sartania, Z. Cheng, M. Lenzner, G. Tempea, Ch. Spielmann, and F. Krausz, "Generation of 0.1-TW 5 fs optical pulses at a 1 kHz repetition rate," Opt. Lett. **22**, 1562–1564 (1997).
10. N. Karasawa, R. Morita, H. Shigekawa, and M. Yamashita, "Generation of intense ultrabroadband optical pulses by induced phase modulation in an argon-filled single-mode hollow waveguide," Opt. Lett. **25**, 183–185 (2000).
11. E. Goulielmakis, S. Koehler, B. Reiter, M. Schultze, A. J. Verhoef, E. E. Serebryannikov, A. M. Zheltikov, and F. Krausz, "Ultrabroadband, coherent light source based on self-channeling of few-cycle pulses in helium," Opt. Lett. **33**, 1407–1409 (2008).
12. A. V. Sokolov, D. R. Walker, D. D. Yavuz, G. Y. Yin, and S. E. Harris, "Raman generation by phased and antiphased molecular states," Phys. Rev. Lett. **85**, 562–565 (2000).
13. S. W. Huang, W. J. Chen, and A. H. Kung, "Vibrational molecular modulation in hydrogen," Phys. Rev. A **74**, 063825 (2006).
14. E. Matsubara, K. Yamane, T. Sekikawa, and M. Yamashita, "Generation of 2.6 fs optical pulses using induced-phase modulation in a gas-filled hollow fiber," J. Opt. Soc. Am. B **24**, 985–989 (2007).
15. K. Hazu, T. Sekikawa, and M. Yamashita, "Spatial light modulator with an over-two-octave bandwidth from ultraviolet to near infrared," Opt. Lett. **32**, 3318–3320 (2007).
16. T. Tanigawa, Y. Sakakibara, S. Fang, T. Sekikawa, and M. Yamashita, "Spatial light modulator of 648 pixels with liquid crystal transparent from ultraviolet to near-infrared and its chirp compensation application," Opt. Lett. **34**, 1696–1698 (2009).
17. G. Sansone, E. Benedetti, F. Calegari, C. Vozzi, L. Avaldi, R. Flammini, L. Poletto, P. Villoresi, C. Altucci, R. Velotta, S. Stagira, S. De Silvestri, and M. Nisoli, "Isolated single-cycle attosecond pulses," Science **314**, 443–446 (2006).
18. E. Goulielmakis, M. Schultze, M. Hofstetter, V. S. Yakovlev, J. Gagnon, M. Uiberacker, A. L. Aquila, E. M. Gullikson, D. T. Attwood, R. Kienberger, F. Krausz, and U. Kleineberg, "Single-cycle nonlinear optics," Science **320**, 1614–1617 (2008).
19. F. Krausz and M. Ivanov, "Attosecond physics," Rev. Mod. Phys. **81**, 163–234 (2009).
20. A. L. Cavalieri, E. Goulielmakis, B. Horvath, W. Helml, M. Schultze, M. Fieb, V. Pervak, L. Veisz, V. S. Yakovlev, M. Uiberacker, A. Apolonski, F. Krausz, and R. Kienberger, "Intense 1.5-cycle near infrared laser waveforms and their use for the generation of ultra-broadband soft-x-ray harmonic continua," New J. Phys. **9**, 242 (2007).
21. F. Quere, J. Itatani, G. L. Yudin, and P. B. Corkum, "Attosecond spectral shearing interferometry," Phys. Rev. Lett. **90**, 073902 (2003).
22. J. Mauritsson, R. Lopez-Martens, A. L'Huillier, and K. J. Schafer, "Ponderomotive shearing for spectral interferometry of extreme-ultraviolet pulses," Opt. Lett. **28**, 2393–2395 (2003).
23. E. Cormier, I. A. Walmsley, E. M. Kosik, A. S. Wyatt, L. Corner, and L. F. DiMauro, "Self-referencing, spectrally, or spatially encoded spectral interferometry for the complete characterization of attosecond electromagnetic pulses," Phys. Rev. Lett. **94**, 033905 (2005).
24. Y. Mairesse, O. Gobert, P. Breger, H. Merdji, P. Meynadier, P. Monchicourt, M. Perdrix, P. Salieres, and B. Carre, "High harmonic XUV spectral phase interferometry for direct electric-field reconstruction," Phys. Rev. Lett. **94**, 173903 (2005).
25. T. Binhammer, E. Rittweger, R. Ell, and F. X. Kartner, "Prism-based pulse shaper for octave spanning spectra," IEEE J. Quantum Electron. **41**, 1552–1557 (2005).
26. T. Binhammer, E. Rittweger, U. Morgner, R. Ell, and F. X. Kartner, "Spectral phase control and temporal superresolution toward the single-cycle pulse," Opt. Lett. **31**, 1552–1554 (2006).

27. Patent by Chisso Corporation, Japan is in progress.
28. K. Oka and T. Kato, "Spectroscopic polarimetry with a channeled spectrum," Opt. Lett. **24**, 1475–1477 (1999).
29. M. Schadt, "Liquid crystal materials and liquid crystal displays," Annu. Rev. Mater. Sci. **27**, 305–379 (1997).
30. Chisso Corporation, Japan (personal communication, 30 October 2009).
31. J. Seres, A. Muller, E. Seres, K. O'Keeffe, M. Lenner, R. F. Kerzog, D. Kaplan, Ch. Spielmann, and F. Krausz, "Sub-10 fs, terawatt-scale Ti:sapphire laser system," Opt. Lett. **28**, 1832–1834 (2003).
32. H. Wang, Y. Wu, C. Li, H. Mashiko, S. Gilbertson, and Z. Chang, "Generation of 0.5 mJ, few-cycle laser pulses by an adaptive phase modulator," Opt. Express **16**, 14448–14455 (2008).